Flexocoupling impact on the generalized susceptibility and soft phonon modes in the ordered phase of ferroics

Anna N. Morozovska,[1,*] Yulian M. Vysochanskii,[2] Oleksandr V. Varenyk,[1] Maxim V. Silibin,[3] Sergei V. Kalinin,[4] and Eugene A. Eliseev[5,†]

[1]*Institute of Physics, National Academy of Science of Ukraine, 46 Prospekt Nauky, 03028 Kyiv, Ukraine*

[2]*Institute of Solid State Physics and Chemistry, Uzhgorod University, 88000 Uzhgorod, Ukraine*

[3]*National Research University of Electronic Technology MIET, Building 1, Shokin Square, 124498, Moscow, Russia*

[4]*The Center for Nanophase Materials Sciences, Oak Ridge National Laboratory, Oak Ridge, Tennessee 37831, USA*

[5]*Institute for Problems of Materials Science, National Academy of Science of Ukraine, 3 Krjijanovskogo, 03142 Kyiv, Ukraine*

(Received 8 July 2015; published 29 September 2015)

The impact of the flexoelectric effect on the generalized susceptibility and soft phonon dispersion is not well known in the long-range-ordered phases of ferroics. Within the Landau-Ginzburg-Devonshire approach we obtained analytical expressions for the generalized susceptibility and phonon dispersion relations in the ferroelectric phase. The joint action of the static and dynamic flexoelectric effects induces nondiagonal components of the generalized susceptibility, whose amplitude is proportional to the convolution of the spontaneous polarization with the flexocoupling constants. The flexocoupling essentially broadens the k spectrum of the generalized susceptibility and leads to an additional "pushing away" of the optical and acoustic soft mode phonon branches. The degeneracy of the transverse optical and acoustic modes disappears in the ferroelectric phase in comparison with the paraelectric phase due to the joint action of flexoelectric coupling and ferroelectric nonlinearity. The results obtained might be mainly important for theoretical analyses of a broad spectrum of experimental data, including neutron and Brillouin scattering.

DOI: 10.1103/PhysRevB.92.094308 PACS number(s): 75.85.+t, 72.80.Vp, 77.84.Ek, 77.80.bn

I. INTRODUCTION

It is difficult to overestimate the significance of the contribution of flexoelectric phenomena to the electromechanics of meso- and especially nanoscale objects, for which strong strain gradients are inevitably present at the surfaces, interfaces, and around point and topological defects [1–3]. According to experiments and Ginzburg-Landau-type theories, flexoelectricity should strongly influence a broad spectrum of local electromechanical responses of spatially inhomogeneous systems with inherent strain and/or polarization gradients. These include flexoelectricity-driven imprinting [4–6] and internal bias in thin films [7,8], the spontaneous flexoelectric effect in nanoferroics [9], and the dead layer effect on ferroelectric thin films conditioned by flexoelectricity [10,11]. Flexoelectric coupling greatly changes the structural, energetic, and electrotransport properties of the domain walls and interfaces in ferroelectrics [12–16] and ferroelastics [17–19], leads to the noticeable hardening of ferroelectrics at nanoindentations [20–22], and significantly affects the local electrochemical strains appearing in response to the excitation of materials with mobile charges by the strongly inhomogeneous electric field of the atomic force microscope tip [23,24] as well as the mechanical writing of ferroelectric polarization by the tip [25]. Notably, flexoelectricity is allowed by symmetry in any material, making the effect widespread and attractive for advanced applications.

Following a classical definition, the static flexoelectric effect is the response of electric polarization to an elastic strain gradient (direct effect), and, vice versa, the polarization appearing as a response to the strain gradient (inverse effect) [7,26–28]. The induced strain is linearly proportional to the polarization gradient $u_{ij}^{sf} = -f_{ijkl}\partial P_k/\partial x_l,$, where f_{ijkl} are the components of the flexocoupling tensor [1–3], and P_k are the polarization components. While the static bulk flexoelectric effect can be viewed as an analog of the piezoelectric effect, the dynamic flexoelectric effect, first introduced by Tagantsev as $P_i^{df} = -M_{ij}\partial^2 U_j/\partial t^2$, where U_j is an elastic displacement and M_{ij} is a flexodynamic tensor, has no such analog, because it corresponds to the polarization response to accelerated motion of the medium in the time domain (see e.g. Refs. [2,3]).

Despite its great importance there are only a few ferroics for which the static flexocoupling tensorial coefficients has been measured experimentally [29–32], obtained from early microscopic estimates [27], or by recent *ab initio* calculations [33,34]. The experimental and theoretical results are rather contradictory, indicating a limited understanding of the effect's nature. The situation with dynamic flexocoupling coefficients is even more unclear. Recently, Kvasov and Tagantsev evaluated the strength of the dynamic flexoelectric effect from *ab initio* calculations and it appeared comparable to that of the static bulk flexoelectric effect [35]. In accordance with this [35] and earlier studies [36,37], an accurate analysis of the soft phonon spectra extracted from the neutron and Brillouin scattering data can provide information about the components of the total flexocoupling coefficient.

It is remarkable that there is an important class of physical problems for which the impact of flexocoupling can be critically important but is not enough studied, and some aspects have been studied rather poorly, including the influence of the static and dynamic flexocouplings on the long-range order parameter fluctuations in the ordered phase of ferroics. Let

*Corresponding author: anna.n.morozovska@gmail.com
†Corresponding author: eugene.a.eliseev@gmail.com

us underline that the basic experimental methods collecting information about the fluctuations are dynamic dielectric measurements and neutron and Brillouin scattering [38–40]. Available experimental and theoretical results (see, e.g., [41–43]) mostly demonstrate the significant material-specific impact of the flexocoupling on the scattering spectra. For instance the theory [36,37] predicts a sharp maximum for $SrTiO_3$ in the field dependence of the dielectric loss due to the significant flexoelectric coupling between the soft mode and acoustic phonon branches, while the analogous field dependence of the loss for $Ba_{0.6}Sr_{0.4}TiO_3$ appeared monotonic because of small flexoelectric coupling.

The impact of the flexoelectric effect on the generalized susceptibility and soft phonon dispersion is not well known theoretically in the long-range-ordered phases of ferroics. This gap in knowledge motivated us to solve the problem for ferroics with local disordering sources (e.g., chemical strains originating from impurity ions or vacancies).

II. GENERAL THEORY: ANALYTICAL RESULTS NEAR THE CENTER OF THE BRILLOUIN ZONE

The generalized expression for the free energy functional has the following form [24]:

$$F = \int_V d^3r \Bigg[\alpha P_i P_i + \alpha_{ijkl} P_i P_j P_k P_l + \alpha_{ijklmn} P_i P_j P_k P_l P_m P_n + \frac{g_{ijkl}}{2}\left(\frac{\partial P_i}{\partial x_j}\frac{\partial P_k}{\partial x_l}\right) - P_i E_i - q_{ijkl} u_{ij} P_k P_l + \frac{c_{ijkl}}{2} u_{ij} u_{kl} + \frac{f_{ijkm}}{2}\left(u_{ij}\frac{\partial P_m}{\partial x_k} - P_m \frac{\partial u_{ij}}{\partial x_k}\right) + [\Xi_{ij}(n - n_e) + \beta_{ij}(N_d^+ - N_{de}^+)] u_{ij} \Bigg]. \quad (1)$$

Hereinafter summation is performed over all repeating indices; P_i is the electric polarization. The expansion coefficient α is temperature dependent, $\alpha = \alpha_T(T - T_C)$, where T is the absolute temperature and T_C is the Curie temperature. The elastic strain tensor is u_{mn}, q_{mnij} is the electrostriction tensor, and f_{mnli} is the flexoelectric effect tensor. The higher-order coefficients α_{ijkl} and α_{ijklmn} are regarded as temperature independent; g_{ijkl} are gradient coefficient tensors**,** and c_{ijkl} are elastic compliances. Also we introduce the fluctuations of the electron density, $\delta n(\mathbf{r}) = n(\mathbf{r}) - n_e$, and donor concentration, $\delta N_d(\mathbf{r}) = N_d^+(\mathbf{r}) - N_{de}^+$, from the space charge equilibrium values n_e and N_{de}^+. The electron density in the conduction band is n and N_d^+ is the concentration of ionized donors, e.g., impurity ions or oxygen vacancies. The deformation potential tensor is denoted by Ξ_{ij} and the Vegard expansion tensor is β_{ij}.

The dynamic equations of state can be derived from the minimization of the Lagrange function $L = F - T$, where the kinetic energy T is given by the expression $T = \frac{\mu}{2}(\frac{\partial P_i}{\partial t})^2 + M_{ij}\frac{\partial P_i}{\partial t}\frac{\partial U_j}{\partial t} + \frac{\rho}{2}(\frac{\partial U_i}{\partial t})^2$,which includes the dynamic flexoelectric coupling with the tensorial strength M_{ij} [2]. U_i is the elastic displacement and ρ is the density of the ferroelectric. The corresponding time-dependent Landau-Ginzburg-Devonshire-type equation of state for ferroelectric polarization reads

$$\mu\frac{\partial^2 P_i}{\partial t^2} + M_{ij}\frac{\partial^2 U_j}{\partial t^2} + 2(\alpha\delta_{ij} - u_{mn}q_{mnij})P_j + 4\alpha_{ijkl}P_j P_k P_l + 6\alpha_{ijklmn}P_j P_k P_l P_m P_n - g_{ijkl}\frac{\partial^2 P_k}{\partial x_j \partial x_l} = f_{mnli}\frac{\partial u_{mn}}{\partial x_l} + E_i. \quad (2)$$

The total field is the sum of depolarization (d) and small probing external (ext) fields, $E_i = E_i^d + \delta E_i^{\text{ext}}$. The field should be found self-consistently from the electric potential ϕ as $E_k = -\partial\phi/\partial x_k$, since the potential satisfies the Poisson equation

$$\varepsilon_b\varepsilon_0\frac{\partial^2\phi}{\partial x_i^2} = \frac{\partial P_i}{\partial x_i} + e(N_d^+ - n), \quad (3)$$

where ε_b is the background permittivity [44] and $\varepsilon_0 = 8.85 \times 10^{-12}$ F/m is the dielectric permittivity of vacuum, $e(N_d^+ - n)$ the space charge density, and $e = 1.6 \times 10^{-19}$ C the electronic charge.

The elastic strains u_{ij} and stresses σ_{ij} are related via the generalized Hooke's law, which includes the conventional Hooke's relation, deformation and chemical stresses, and flexoelectric and electrostriction terms [23,24]. Since the time-dependent equation of mechanical equilibrium, $\partial\sigma_{ij}/\partial x_j = \rho\partial^2 U_i/\partial t^2$, should be valid, the equation transforms into a dynamic Lamé-type equation for elastic strain

$$c_{ijkl}\frac{\partial^2 U_l}{\partial x_j \partial x_k} - \rho\frac{\partial^2 U_i}{\partial t^2} - M_{ij}\frac{\partial^2 P_j}{\partial t^2} = -\frac{\partial}{\partial x_j}\left(\Xi_{ij}\delta n + \beta_{ij}\delta N_d + f_{ijkl}\frac{\partial P_l}{\partial x_k} - q_{ijkl}P_k P_l\right). \quad (4)$$

In order to derive expression for the linear generalized susceptibility and the correlation function, let us linearize Eq. (2) for polarization and Eq. (4) for the displacement in the vicinity of the spontaneous values $u_{kl} = u_{kl}^{(s)} + \delta u_{kl}$ and $P_i = P_i^{(s)} + \delta P_i$, where $u_{mn}^{(s)} = s_{mnij}q_{ijkl}P_k^{(s)}P_l^{(s)}$ is the spontaneous strain related to the spontaneous polarization $P_l^{(s)}$. Both spontaneous strain and polarization are supposed to be coordinate and time independent in the considered bulk system. The electric field $E_i = E_i^{(s)} + \delta E_i^d + \delta E_i^{\text{ext}}$, where the depolarization field fluctuations δE_i^d will be estimated in the Debye approximation as described in Appendix A of the Supplemental Material [45].

The Fourier representations in the spatial k and frequency ω domains of the linearized solution for polarization and strain

fluctuation have the forms

$$\delta\tilde{P}_j(\mathbf{k},\omega) = \left[\delta\tilde{E}_i^{\text{ext}} + ik_{j'}S_{mi'}(\mathbf{k},\omega)\left(2ik_nq_{mnij}P_j^{(s)} + f_{mnli}k_lk_n - M_{mi}\omega^2\right)\delta\tilde{C}_{i'j'}\right]\tilde{\chi}_{ij}(\mathbf{k},\omega), \tag{5a}$$

$$\delta\tilde{U}_k(\mathbf{k},\omega) = -ik_j\delta\tilde{C}_{ij}S_{ik}(\mathbf{k},\omega) + S_{ik}(\mathbf{k},\omega)\tilde{\chi}_{sl}(\mathbf{k},\omega)\left(f_{ijml}k_jk_m - M_{il}\omega^2 - 2ik_jq_{ijnl}P_n^{(s)}\right) \times\left[\delta\tilde{E}_s^{\text{ext}} + i\left(f_{qnps}k_pk_n - M_{qs}\omega^2\right)k_{j'}S_{qi'}(\mathbf{k},\omega)\delta\tilde{C}_{ij}\right], \tag{5b}$$

where $\delta\tilde{C}_{ij} = (\Xi_{ij}\delta\tilde{n} + \beta_{ij}\delta\tilde{N}_d)$. Since the harmonic approach (5) is applicable for small wave vector **k,** we would like to underline that we did not aim to reach quantitative agreement between the calculated and experimentally observed soft phonon spectra in the entire first Brillouin zone. Consideration of the problem for higher **k** values requires inclusion of the anharmonicity and higher gradient terms [46].

The generalized susceptibility $\tilde{\chi}_{ij}(\mathbf{k},\omega)$, which is in fact the correlation function, and the elastic function $S_{ir}(\mathbf{k},\omega)$ included in Eqs. (5) are given by the expressions

$$\tilde{\chi}_{ij}^{-1}(\mathbf{k},\omega) = \beta_{ij}(\mathbf{k},\omega) + \Theta_{ipjl}(\mathbf{k},\omega) + Q_{ij}(\mathbf{k},\omega) + \gamma_{ijkl}(\mathbf{k},\omega)P_k^{(s)}P_l^{(s)}, \tag{6a}$$

$$S_{ik}^{-1}(\mathbf{k},\omega) = c_{ijkl}k_lk_j - \rho\omega^2\delta_{ik}. \tag{6b}$$

Here the linear dynamic stiffness is affected by the depolarization effect as $\beta_{ij}(\mathbf{k},\omega) = (2\alpha - \mu\omega^2)\delta_{ij} + \frac{k_ik_j}{\varepsilon_b\varepsilon_0(k^2+R_d^{-2})}$, where R_d is the Debye screening radius. The nonlinear stiffness is $\gamma_{ijkl}(\mathbf{k},\omega) = 12\alpha_{ijkl} - 2q_{mnij}q_{i'j'kl}s_{mni'j'} - 4q_{mnil}q_{i'j'jk}k_{j'}k_nS_{mi'}(\mathbf{k},\omega) + 30\,\alpha_{ijklmn}P_m^{(s)}P_n^{(s)}$. The flexoelectric coupling changes the polarization gradient coefficient tensor g_{ipjl} to an ω- and k-dependent tensorial function that has the following form $\Theta_{ipjl}(\mathbf{k},\omega) = g_{ipjl}k_pk_l - (f_{mnli}k_nk_l - M_{mi}\omega^2)(f_{i'j'pj}k_{j'}k_p - M_{i'j}\omega^2)S_{mi'}(\mathbf{k},\omega)$. The additional complex term $Q_{ij}(\mathbf{k},\omega)$ is proportional to the convolution of the spontaneous polarization vector with the static and dynamic flexocoupling constants:

$$Q_{ij}(\mathbf{k},\omega) = 2iS_{mi'}(\mathbf{k},\omega)[(f_{mnpi}k_pk_n - M_{mi}\omega^2)k_{j'}q_{i'j'kj} - (f_{i'j'pj}k_pk_{j'} - M_{i'j}\omega^2)k_nq_{mnik}]P_k^{(s)}. \tag{7}$$

Here the static and dynamic flexocoupling appeared in a universal combination $(f_{mnpi}k_pk_n - M_{mi}\omega^2)$. The term is absent in a paraelectric phase, since there $P_k^{(s)} = 0$.

Note that the Green tensor $\tilde{\chi}_{ij}(\mathbf{k},\omega)$ is independent of any source of the fluctuations by definition. However, polarization variation $\delta\tilde{P}_j(\mathbf{k},\omega)$ and displacement variation $\delta\tilde{U}_k(\mathbf{k},\omega)$, which are the solutions of the linearized equations (5), are proportional to both sources, the external electric field variation $\delta\tilde{E}_i^{\text{ext}}$ and the concentration disorder $\delta\tilde{C}_{ij}$, but the proportionality coefficients are different in nature. In particular the relation $\delta\tilde{P}_j(\mathbf{k},\omega) \sim \delta\tilde{E}_i^{\text{ext}}\tilde{\chi}_{ij}(\mathbf{k},\omega)$ is conventional and means that the polarization fluctuation is proportional to the dielectric susceptibility, but it is partly proportional to another source $\delta\tilde{P}_j(\mathbf{k},\omega) \sim ik_{j'}S_{mi'}(\mathbf{k},\omega)(2ik_nq_{mnij}P_j^{(s)} + f_{mnli}k_lk_n - M_{mi}\omega^2)\tilde{\chi}_{ij}(\mathbf{k},\omega)\delta\tilde{C}_{i'j'}$, which looks nontrivial due to the presence of additional electrostrictive and static and dynamic flexocoupling contributions $(2ik_nq_{mnij}P_j^{(s)} + f_{mnli}k_lk_n - M_{mi}\omega^2)$.

The order parameter correlation function is related to the generalized susceptibility via the Callen-Welton fluctuation-dissipation theorem [47] and the corresponding correlation radius can be determined from the direct matrix $\tilde{\chi}_{ij}(\mathbf{k},\omega)$. Following the Cochren paper [38], the dynamical structural factor of neutron scattering is proportional to the dynamic susceptibility spectrum $\tilde{\chi}(\mathbf{k},\omega)$. The integrated intensity of the scattering is proportional to the static spectrum $(d\sigma/d\Omega) \sim \tilde{\chi}(\mathbf{k},0)$. In the next section we discuss the influence of the flexocoupling on the static spectrum of the dielectric susceptibility in a ferroelectric phase.

III. FLEXOCOUPLING IMPACT ON THE DYNAMIC GENERALIZED SUSCEPTIBILITY IN A FERROELECTRIC PHASE

In the general case analytical expressions for $\tilde{\chi}_{ij}(\mathbf{k},\omega)$ are rather cumbersome. In order to analyze analytically concrete cases, below we consider a uniaxial ferroelectric with a spontaneous polarization directed along the z axis, $\mathbf{P}^{(s)} = (0,0,P_S)$ and other tensorial properties (elastic, electrostrictive, and flexoelectric) in the cubic symmetry approximation. Analytical results were derived for the basic orientations of the wave vector $\mathbf{k} = (0,0,k_z)$ and $\mathbf{k} = (k_x,0,0)$ [or $\mathbf{k} = (0,k_y,0)$]. Calculation details are listed in Appendix B of the Supplemental Material [45]. All numerical calculations in this and the next sections are performed for $PbZr_{0.4}Ti_{0.6}O_3$ (PZT) in its cubic paraelectric and tetragonal ferroelectric phases.

A. Orientation I of the wave vector k = (0,0,k_z): Ferroelectric phase

For the case, when a wave vector $\mathbf{k} = (0,0,k_z)$ is parallel to the spontaneous polarization direction $\mathbf{P}_S = (0,0,P_S)$, the corresponding nonzero components of the susceptibility are [45]

$$\tilde{\chi}_{11}(\mathbf{k},\omega) = \tilde{\chi}_{22}(\mathbf{k},\omega) = \frac{1}{\alpha_{11}^* - \mu\omega^2 + g_{44}^*k_z^2}, \tag{8a}$$

$$\tilde{\chi}_{33}(\mathbf{k},\omega) = \left(\alpha_{33}^* - \mu\omega^2 + g_{11}^*k_z^2 + \frac{k_z^2}{\varepsilon_b\varepsilon_0\left(k_z^2 + R_d^{-2}\right)}\right)^{-1}. \tag{8b}$$

Hereinafter the Voigt notations are used. The spontaneous polarization contributes to the spectrum of $\tilde{\chi}_{ij}(\mathbf{k},\omega)$ via the renormalization of the dielectric stiffness coefficient α as $\alpha_{11}^*(\mathbf{k},\omega) = 2\alpha + P_S^2(\beta_{12}^* - \frac{q_{44}^2k_z^2}{c_{44}k^2-\rho\omega^2}) + 2\alpha_{112}P_S^4$ and $\alpha_{33}^*(\mathbf{k},\omega) = 2\alpha + P_S^2(\beta_{11}^* - \frac{4q_{11}^2k_z^2}{c_{11}k_z^2-\rho\omega^2}) + 30\alpha_{111}P_S^4$. The nonlinear stiffness α_{ijkl} is renormalized by electrostriction

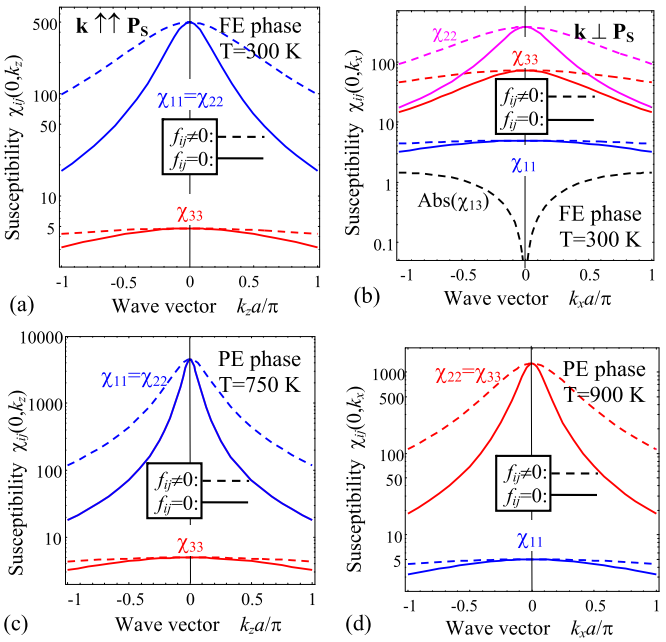

FIG. 1. (Color online) Spatial spectrum of the generalized susceptibility nonzero components $\tilde{\chi}_{ij}(\omega=0,k_x)$ calculated for the different directions of fluctuation of the wave vector $\mathbf{k}$ with respect to the spontaneous polarization $\mathbf{P}_S=(0,0,P_S)$. (a) $\vec{k}\uparrow\uparrow\vec{P}_S$ and transverse (b) $\vec{k}\perp\vec{P}_S$. a is the lattice constant; temperature $T=300$ K corresponds to the ferroelectric phase (legend "FE"). (c),(d) are calculated in the paraelectric phase (legend "PE") at temperatures $T=750$ K (c) and $T=900$ K (d). Dashed curves are calculated with flexoelectric effect (legend "$f_{ij}\neq 0$") and solid curves are without it (legend "$f_{ij}=0$"). The curves are calculated for PZT parameters from Table I.

coupling as $\beta^*_{11}=12\alpha_{11}-\frac{2(q_{11}+2q_{12})^2}{3(c_{11}+2c_{12})}-\frac{2q_{44}^2}{3c_{44}}$ and $\beta^*_{12}=2\alpha_{12}-\frac{2(q_{11}+2q_{12})^2}{3(c_{11}+2c_{12})}+\frac{q_{44}^2}{3c_{44}}$.Thus the contribution of spontaneous polarization via the ferroelectric nonlinearity ($\sim\beta^*_{12}P_S^2$) and electrostriction ($\sim q_{ij}q_{kj}P_S^2$) mechanisms can lead to either increase or decrease of the coefficients α^*_{ij} depending on the signs of the material constants.

Flexocoupling changes the gradient coefficients as

$$g^*_{11}(\mathbf{k},\omega)=g_{11}-\frac{\left(f_{11}k_z^2-M_{11}\omega^2\right)^2}{k_z^2\left(c_{11}k_z^2-\rho\omega^2\right)},$$
$$g^*_{44}(\mathbf{k},\omega)=g_{44}-\frac{\left(f_{44}k_z^2-M_{11}\omega^2\right)^2}{k_z^2\left(c_{44}k_z^2-\rho\omega^2\right)}. \tag{9}$$

The term $(\varepsilon_b\varepsilon_0)^{-1}k_z^2/(k_z^2+R_d^{-2})$ in $\tilde{\chi}_{33}$ originates from the depolarization electric field.

The static k-spectra of $\tilde{\chi}_{ij}(\mathbf{k},0)$ calculated in the ferroelectric phase with and without the flexocoupling contribution are shown in Fig. 1(a). The component $\tilde{\chi}_{33}$ is much smaller than the ones due to the depolarization effect. As one can see from the figure, the flexoelectric effect essentially broadens the k spectrum of all susceptibility components and the broadening increases with increase of k. Both spectra coincide at the point $\mathbf{k}=\mathbf{0}$ as anticipated. The dynamic flexoeffect does not contribute to the spectra in the static case ($\omega=0$). The contribution of spontaneous polarization via the ferroelectric nonlinearity and electrostriction mechanisms can lead to both broadening and narrowing of the different components of the susceptibility k spectra.

B. Orientation II of the wave vector $\mathbf{k}=(k_x,0,0)$: Ferroelectric phase

For the case when a fluctuation wave vector $\mathbf{k}=(k_x,0,0)$ is normal to the spontaneous polarization direction $\mathbf{P}_S=(0,0,P_S)$, the corresponding nonzero components of the generalized susceptibility are [45]

$$\tilde{\chi}_{11}(\mathbf{k},\omega)=\frac{\alpha^*_{11}-\mu\omega^2+g^*_{44}k_x^2}{\Delta_{22}(\mathbf{k},\omega)},\quad \tilde{\chi}_{22}(\mathbf{k},\omega)=\frac{1}{\alpha^*_{22}-\mu\omega^2+g^*_{44}k_x^2}, \tag{10a}$$

$$\tilde{\chi}_{33}(\mathbf{k},\omega)=\left(\alpha^*_{33}-\mu\omega^2+g^*_{11}k_x^2+\frac{k_x^2}{\varepsilon_b\varepsilon_0\left(k_x^2+R_d^{-2}\right)}\right)\frac{1}{\Delta_{22}(\mathbf{k},\omega)}, \tag{10b}$$

$$\tilde{\chi}_{13}(\mathbf{k},\omega)=-\tilde{\chi}_{31}(\mathbf{k},\omega)=\frac{-2iP_Sk_x}{\Delta_{22}(\mathbf{k},\omega)}\left(\frac{q_{12}\left(f_{11}k_x^2-M_{11}\omega^2\right)}{c_{11}k_x^2-\rho\omega^2}-\frac{q_{44}\left(f_{44}k_x^2-M_{11}\omega^2\right)}{2\left(c_{44}k_x^2-\rho\omega^2\right)}\right). \tag{10c}$$

The spontaneous polarization contributes to the components by the renormalization of the linear dielectric stiffness coefficients $\alpha^*_{11}(\mathbf{k},\omega)=2\alpha+(\beta^*_{11}-\frac{4q_{12}{}^2k_x^2}{c_{11}k_x^2-\rho\omega^2})P_S^2+30\alpha_{111}P_S^4$, $\alpha^*_{22}(\mathbf{k},\omega)=2\alpha+\beta^*_{12}P_S^2+2\alpha_{112}P_S^4$, and $\alpha^*_{33}(\mathbf{k},\omega)=2\alpha+(\beta^*_{12}-\frac{q_{44}^2k_x^2}{c_{44}k_x^2-\rho\omega^2})P_S^2+2\alpha_{112}P_S^4$.The forms of the gradient functions $g^*_{11}(\mathbf{k},\omega)$ and $g^*_{44}(\mathbf{k},\omega)$ used in Eqs. (10) are the same as those in Eq.(9) with the only substitution $k_z\to k_x$. Note that the nonzero nondiagonal element $\tilde{\chi}_{13}(\mathbf{k},\omega)$ is proportional to the product of the spontaneous polarization value and the flexocoupling constants. The denominator $\Delta_{22}(\mathbf{k},\omega)$ is expressed in terms

of inverse matrix elements, $\Delta_{22}(\mathbf{k},\omega) = \tilde{\chi}_{11}^{-1}(\mathbf{k},\omega)\tilde{\chi}_{33}^{-1}(\mathbf{k},\omega) - \tilde{\chi}_{13}^{-1}(\mathbf{k},\omega)\tilde{\chi}_{31}^{-1}(\mathbf{k},\omega)$. The evident expression for $\Delta_{22}(\mathbf{k},\omega)$ is

$$\Delta_{22}(\mathbf{k},\omega) = s - 4k_x^2 P_S^2\left(\frac{q_{12}\left(f_{11}k_x^2 - M_{11}\omega^2\right)}{c_{11}k_x^2 - \rho\omega^2} - \frac{q_{44}\left(f_{44}k_x^2 - M_{11}\omega^2\right)}{2\left(c_{44}k_x^2 - \rho\omega^2\right)}\right)^2 \cdot$$
$$+\left(\alpha_{11}^* - \mu\omega^2 + g_{44}^* k_x^2\right)\left(\alpha_{33}^* - \mu\omega^2 + g_{11}^* k_x^2 + \frac{k_x^2}{\varepsilon_b\varepsilon_0\left(k_x^2 + R_d^{-2}\right)}\right) \quad (11)$$

The flexocoupling induces several major changes in the susceptibilities, in particular to the terms directly proportional to the product of spontaneous polarization and flexocoupling constants originating from $\tilde{\chi}_{13}(\mathbf{k},\omega)$, as well as changes related to the gradient functions $g_{ii}^*(\mathbf{k},\omega)$. The physical interpretation of the nondiagonal components of the susceptibility given by Eq. (10c) seems very important for us, because it can stimulate experimental verification of the theoretical prediction. The appearance of $\tilde{\chi}_{13}(\mathbf{k},\omega) = -\tilde{\chi}_{31}(\mathbf{k},\omega)$ in a ferroelectric with noticeable flexocoupling means that the application of a spatially inhomogeneous probing electric field in direction 3 (or 1) should induce a polarization change in direction 1 (or 3), and that the frequency spectrum is proportional to the product of the spontaneous polarization value P_S and factors proportional to the static and dynamic flexocoupling constants. We may suggest performing experiments aimed at studying the changes of the nondiagonal components of the dielectric permittivity tensor induced by spatially modulated electromagnetic waves (such as induced optical gyration) or by an electric field gradient in the ferroelectric phase of those ferroics whose dielectric response to a homogeneous electric field does not contain any nondiagonal contributions.

The static $\mathbf{k}$-spectra of $\tilde{\chi}_{ij}(\mathbf{k},0)$ calculated in the ferroelectric phase with and without flexocoupling contributions are shown in the Fig. 1(b). The strict inequalities $\tilde{\chi}_{11} \ll \tilde{\chi}_{33} \ll \tilde{\chi}_{22}$ and $|\tilde{\chi}_{13}| \ll \tilde{\chi}_{33}$ are valid due to the depolarization effect, because the denominator $\Delta_{22}(\mathbf{k},0)$ includes the depolarization factor $(\varepsilon_b\varepsilon_0)^{-1}k^2/(k^2 + R_d^{-2})$ and thus strongly decreases $\tilde{\chi}_{11}$, $\tilde{\chi}_{13}$, and $\tilde{\chi}_{33}$ in comparison with the component $\tilde{\chi}_{22}$, which is not affected by depolarizing at all, as should be expected for transverse fluctuations of the polarization z component in the direction 1. Since $\tilde{\chi}_{33}$ contains the depolarization factor in the numerator, it becomes much higher than the components $\tilde{\chi}_{11}$ and $\tilde{\chi}_{13}$. As one can see from Fig. 1(b) the flexoelectric effect induces the nondiagonal component $\tilde{\chi}_{13}$, which is odd with respect to $\mathbf{k}$, and essentially broadens the k spectrum of the diagonal components of the susceptibility. The broadening increases with increase of k.

C. Paraelectric phase

Finally, let us compare the susceptibility spectrum in the ferroelectric and paraelectric phases. Corresponding expressions in the paraelectric phase can be derived from Eqs. (8)–(11) at $\mathbf{P}_S = \mathbf{0}$. Since the determinant $\Delta_{22}(\mathbf{k},\omega) = (\alpha_{11}^* - \mu\omega^2 + g_{44}^* k_x^2)(\alpha_{33}^* - \mu\omega^2 + g_{11}^* k_x^2 + \frac{k_x^2}{\varepsilon_b\varepsilon_0(k_x^2+R_d^{-2})})$ and the susceptibility component $\tilde{\chi}_{13}(\mathbf{k},\omega) = -\tilde{\chi}_{31}(\mathbf{k},\omega) = 0$ in the paraelectric phase, the mathematical forms of the expressions obtained coincide with Eqs. (8). Thus three diagonal components are nonzero in the paraelectric phase, but only two of them are different. The static $\mathbf{k}$ spectra of $\tilde{\chi}_{ij}(\mathbf{k},0)$ calculated in the paraelectric phase with and without the flexocoupling contribution are shown in Figs. 1(c) and 1(d) for two different temperatures $T = 750$ K (c) and 900 K (d). Both paraelectric spectra look similar to the ferroelectric one calculated for the case $\vec{k}\uparrow\uparrow\vec{P}_S$ and shown in Fig. 1(a). When the temperature approaches the phase transition at $T = 691$K the maximum height strongly increases for some of the susceptibility components, namely, $\tilde{\chi}_{11}(0,k_z) = \tilde{\chi}_{22}(0,k_z)$ increases for the case $\mathbf{k} = (0,0,k_z)$ and $\tilde{\chi}_{22}(0,k_x) = \tilde{\chi}_{33}(0,k_x)$ increases for the case $\mathbf{k} = (k_x,0,0)$, as anticipated [compare the vertical scales in Figs. 1(c) and 1(d)].

The condition for the onset of the homogeneous distribution instability follows from the analysis of the determinant $\det[\tilde{\chi}_{ij}^{-1}(\mathbf{k},\omega)] = 0$. In the static limit ($\omega = 0$) and in the paraelectric phase the condition reduces to the following equations:

$$2\alpha c_{44} + k^2\left(c_{44}g_{44} - f_{44}^4\right) = 0,$$
$$\left(2\alpha + \frac{k^2}{\varepsilon_b\varepsilon_0\left(k^2 + R_d^{-2}\right)}\right)c_{11} + k^2\left(c_{11}g_{11} - f_{11}^4\right) = 0. \quad (12a)$$

The derivation details of Eq. (12a) are listed in Appendix C of the Supplemental Material [45]. Since the coefficient α is not negative in a paraelectric phase and the factor $1/\varepsilon_b\varepsilon_0(k_x^2 + R_d^{-2})$ is positive, Eqs. (12a) give sufficient conditions for homogeneous distribution stability:

$$f_{11}{}^2 < g_{11}c_{11}, \quad f_{44}{}^2 < g_{44}c_{44}. \quad (12b)$$

Note that the condition $f_{44}{}^2 < g_{44}c_{44}$ coincides with the one derived in Refs. [9,48]. If one of the inequalities (12b) becomes invalid, one can expect the onset and evolution of the modulated phases.

The tensor R_{ij} of correlation radii is proportional to the second derivative of the generalized susceptibility, $R_{ij}^2 = -\frac{1}{2\tilde{\chi}_{ij}}\left(\frac{\partial^2\tilde{\chi}_{ij}(\mathbf{k},0)}{\partial k^2}\right)^2|_{k\to 0}$,where $\mathbf{k}$ is either k_z or k_x. The dependences of the correlation radii of R_{ij} on the flexoelectric coefficients f_{11} and f_{44} are shown in Figs. 2(a) and 2(b), respectively. The correlation radii either monotonically decrease with increase of the flexoelectric coupling constants f_{ij} or remained independent of some f_{ij}. In particular R_{13} always decreases with increase of f_{ij}, because $\tilde{\chi}_{13}$ is proportional to f_{ij}. The situation with other R_{ij} depends on the orientation of the vector $\mathbf{k}$ with respect to the spontaneous polarization $\mathbf{P}_S$.

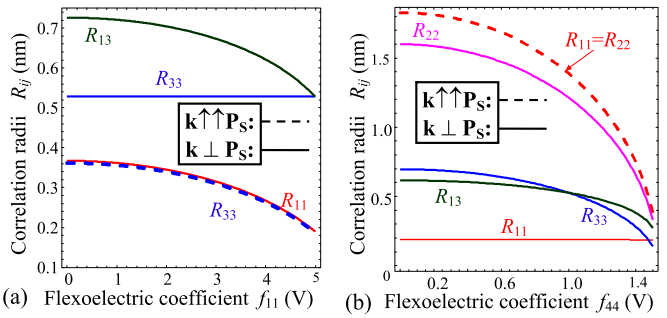

FIG. 2. (Color online) Dependence of correlation radii R_{ij} on the flexoelectric coefficient f_{11} (a) and f_{44} (b). Dashed curves are calculated for $\vec{k}\uparrow\uparrow\vec{P}_S$ and solid curves correspond to $\vec{k}\perp\vec{P}_S$. The curves are calculated for PZT parameters from Table I. Temperature $T = 300\,\mathrm{K}$.

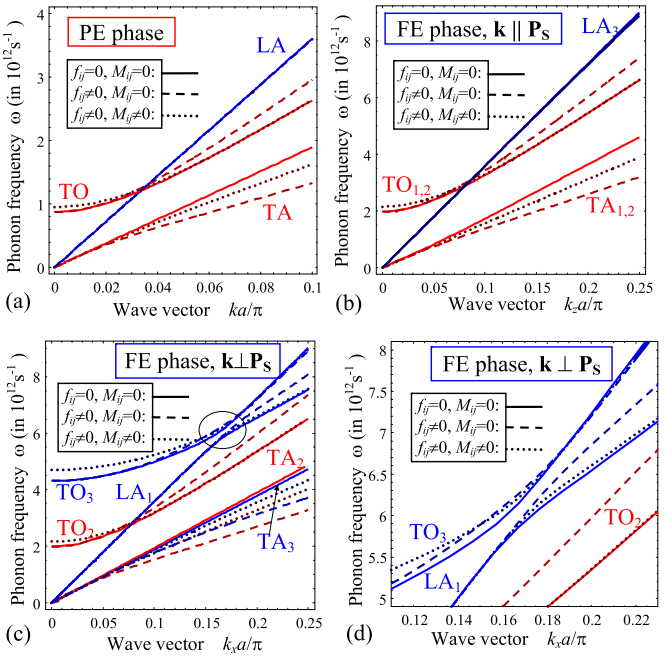

FIG. 3. (Color online) Soft phonon frequency dispersion. The wave vector $\mathbf{k}$ is reduced in π/a units; a is the lattice constant. (a) corresponds to the paraelectric phase (legend "PE") of PZT at temperature $T = 700\,\mathrm{K}$; (b) and (c) are calculated in the ferroelectric phase (legend "FE") at temperature $T = 680\,\mathrm{K}$ for longitudinal $\vec{k}\uparrow\uparrow\vec{P}_S$ (b) and transverse $\vec{k}\perp\vec{P}_S$ (c),(d) fluctuation of the wave vector direction with respect to the spontaneous polarization $\mathbf{P}_S = (0,0,P_S)$. Solid curves are calculated without flexoelectric coupling (legend "$f_{ij} = 0, M_{ij} = 0$"); dashed curves are calculated with the static but without the dynamic coupling (legend "$f_{ij}\neq0, M_{ij} \neq 0$"); dotted curves are calculated with the dynamic and static flexoelectric couplings included (legend "$f_{ij} \neq 0, M_{ij} \neq 0$"). (d) Zoom of the plot (c) inside the circle. The curves are calculated for PZT parameters from Table I.

IV. THE IMPACT OF FLEXOCOUPLING ON SOFT PHONON SPECTRA

Starting from the classic Shirane *et al.* papers [41–43], soft phonon dispersion has been studied experimentally for several incipient and actual ferroelectrics. Below we study the impact of the flexocoupling on the soft phonon dispersion in the ferroelectric phase and compare the results with those in a paraelectric phase.

Dispersion relations for longitudinal and transverse optical (LO and TO) and acoustic (LA and TA) modes can be obtained from analyses of the determinant $\det[\tilde{\chi}_{ij}^{-1}(\mathbf{k},\omega)] = 0$. Dispersion relations for the direction of the fluctuation wave vector $\mathbf{k} = (0,0,k_z)$ were derived for the cases $\mathbf{k}\uparrow\uparrow\delta P$ and $\mathbf{k}\perp\delta P$, respectively. They acquire the forms

$$\begin{pmatrix} 2\alpha - \mu\omega^2 + g_{11}k_z^2 - \frac{\left(f_{11}k_z^2 - M_{11}\omega^2\right)^2}{c_{11}k_z^2 - \rho\omega^2} + \frac{k_z^2}{\varepsilon_b\varepsilon_0\left(k_z^2 + R_d^{-2}\right)} \\ + P_S^2\left(\beta_{11}^* - \frac{4q_{11}^2k_z^2}{c_{11}k_z^2 - \rho\omega^2}\right) + 30\alpha_{111}P_S^4 \end{pmatrix} = 0, \tag{13a}$$

$$2\alpha - \mu\omega^2 + g_{44}k_z^2 - \frac{\left(f_{44}k_z^2 - M_{11}\omega^2\right)^2}{c_{44}k_z^2 - \rho\omega^2} + P_S^2\left(\beta_{12}^* - \frac{q_{44}^2k_z^2}{c_{44}k_z^2 - \rho\omega^2}\right) + 2\alpha_{112}P_S^4 = 0. \tag{13b}$$

The dispersion relation for the direction of the fluctuation wave vector $\mathbf{k} = (k_x,0,0)$ has the form

$$\left[2\alpha - \mu\omega^2 + g_{44}^*(\mathbf{k},\omega)k_x^2 + P_S^2\beta_{12}^*\right]\Delta_{22}(\mathbf{k},\omega) = 0. \tag{13c}$$

The terms originating from the static and dynamic flexocoupling appeared in the combinations $(f_{11}k_z^2 - M_{11}\omega^2)$ and $(f_{44}k_z^2 - M_{11}\omega^2)$ in the equations. The spontaneous polarization P_S, via the ferroelectric nonlinearity and electrostriction mechanisms, generates the terms proportional to $\beta_{ij}^*P_S^2$, $\alpha_{ijkl}P_S^4$, and $q_{ij}q_{kj}P_S^2$ in the equations. Due to the k dependence of the terms $\sim P_S^2$ an analytical solution of Eqs. (13) is absent in the ferroelectric phase.

The features of the soft phonon k spectra were calculated with static ($f_{ij} \neq 0$ and $M_{ij} = 0$) and dynamic ($f_{ij} \neq 0$ and $M_{ij} \neq 0$) flexocoupling and without it ($f_{ij} = 0$ and $M_{ij} = 0$). Spectra calculated in the paraelectric and ferroelectric phases for the cases $\vec{k}\uparrow\uparrow\vec{P}_S$ and $\vec{k}\perp\vec{P}_S$ are compared in Figs. 3(a), 3(b), and 3(c), respectively. Parameters corresponding to PZT are listed in Table I.

Equations (13) have relatively simple analytical solutions in a paraelectric phase ($P_S^2 = 0$), namely, two acoustic (LA and TA) and two optical (LO and TO) modes [see Fig. 3(a)]. Equation (13a) has an analytical solution in a ferroelectric phase also, and it contains one acoustic mode LA_3 and a very high longitudinal optical mode (LO) with frequency at about $150 \times 1012\,\mathrm{s}^{-1}$, which is maximal in the dielectric limit ($R_d^{-2} \to 0$). The LO mode is weakly dependent on temperature due to the depolarization factor $k_z^2/\varepsilon_b\varepsilon_0(k_z^2 + R_d^{-2})$, which becomes extremely large in the dielectric limit. Both paraelectric and ferroelectric spectra contain rather high-frequency longitudinal optical modes (LO) due to the strong depolarization field, which is maximal in the dielectric limit and is almost independent of the flexocouplings and temperature. Therefore the LO modes are not shown in Fig. 3. The longitudinal soft mode LA_3 is insensitive to the flexocoupling, because its dispersion is strongly affected by the depolarization.

TABLE I. Material parameters for bulk ferroelectric.

Coefficient	$PbZr_{0.4}Ti_{0.6}O_3$ (from [49,50])	$PbTiO_3$ (from [51])
ε_b	5 [44]	5
$\alpha_{iT}(10^5 C^{-2}\,mJ/K)$	2.12	3.765
$T_C(K)$	691	752
$\alpha_{ij}^{(\sigma)}(10^8 C^{-4} m^5 J)$	$a_{11}=0.3614$, $a_{12}=3.233$	$a_{11}=-0.725$, $a_{12}=7.50$
$\alpha_{ijk}(10^8 J\,m^9 C^{-6})$	$a_{111}=1.859$, $a_{112}=8.503$, $a_{123}=-40.63$	$a_{111}=2.606$, $a_{112}=6.10$, $a_{123}=-36.60$
$q_{ij}(10^9 V\,m/C)$	$q_{11}=8.91$, $q_{12}=-0.787$, $q_{44}=3.18$	$q_{11}=11$, $q_{44}=7$
$c_{ij}(10^{10} Pa)$	$c_{11}=17.0$, $c_{12}=8.2$, $c_{44}=4.7$	$c_{11}=18$, $c_{12}=7.9$, $c_{44}=11$
$g_{ij}(10^{-10} C^{-2}\,m^3\,J)$	$g_{11}=2.0$, $g_{44}=1.0$[a]	$g_{11}=1.5$, $g_{44}=0.5$
$f_{ij}(V)$	$f_{11}=5$, $f_{12}=-1$, $f_{44}=+1$[b]	$f_{11}=-8$, $f_{44}=-1.9$
$M_{11}(Vs^2/m^2)$	6×10^{-8} [35]	-2×10^{-8}
$\rho(10^3 kg/m^3)$	8.087[c]	7.986
$\mu\,(10^{-18} s^2 mJ)$	1.413 [41]	1.59
$R_d(m)$	From 20 nm to infinity	Infinity

[a]Estimated from domain wall width.
[b]Estimated from [27,30,31,32].
[c]At normal conditions.

Due to the k dependence of the terms $\sim P_S^2$ an analytical solution of Eqs. (13b) is absent in a ferroelectric phase. The corresponding numerical solution has four degenerate transverse soft phonon branches, namely, two optical ($TO_1 = TO_2$) and two acoustic ($TA_1 = TA_2$) modes [see Fig. 3(b)]. All the transverse soft modes are relatively sensitive to both dynamic and static flexocoupling constants, especially at $k_z a/\pi \geqslant 0.03$, where a is the lattice constant [compare the solid, dotted, and dashed curves for TO modes in Figs. 3(a) and 3(b)]. Since the calculated phonon spectrum in the paraelectric phase has two acoustic (LA and TA) and two optical (LO and TO) modes, we can conclude that the appearance of spontaneous polarization does not lead to qualitative changes in the spectra for the case of wave vector direction $\vec{k}\uparrow\uparrow\vec{P}_S$.

Without flexocoupling the numerical solution of Eq. (13c) has six different phonon branches in the ferroelectric phase for the case $\vec{k}\perp\vec{P}_S$, namely, three optical (LO, TO_2, and TO_3) and three acoustic (LA_1, TA_2, and TA_3) modes; the frequencies of the modes TA_2 and TA_3 are almost the same at $ka_x/\pi < 0.3$ [see the solid curves in Fig. 3(c)]. With the flexocoupling included, the solution in the ferroelectric phase has also six different soft phonon branches, three optical (LO, TO_2, and TO_3) and three acoustic (LA_1, TA_2, and TA_3) modes; in this case the frequencies of the modes TA_2 and TA_3 are noticeably different at $ka_x/\pi < 0.3$ [see the dashed and dotted curves in Fig. 3(c)]. Since the phonon spectra in the paraelectric phase have two optical (LO and TO) and two acoustic (LA and TA) modes [see Fig. 3(a)], we can conclude that the appearance of spontaneous polarization leads to the removal of the degeneracy of the acoustic and optical modes TA and TO for the case $\vec{k}\perp\vec{P}_S$ and consequently to the appearance of different transverse acoustic and optical modes TA_2 and TA_3, TO_2 and TO_3. The transverse $TO_{2,3}$ and $TA_{2,3}$ modes are relatively sensitive to both the static and dynamic flexoelectric coupling strength for the case $\vec{k}\perp\vec{P}_S$ and $k_x a/\pi \geqslant 0.1$ for acoustic modes and for small k for optical modes; meanwhile the longitudinal LA_1 mode becomes sensitive to the coupling at $k_x a/\pi \geqslant 0.15$ [compare the solid, dotted, and dashed curves in Fig. 3(c)]. The flexoelectric coupling significantly increases the splitting of the TA_2 and TA_3 modes. Moreover, the TO_3 and LA_1 modes are "pushed away" by the static and dynamic flexocoupling in the ferroelectric phase at small **k** ($k_x a/\pi \leqslant 0.15$) and start to approach each other at $k_x a/\pi \geqslant 0.15$ [compare the solid and dashed curves in Fig. 3(d)]. The effects give us the opportunity to define the static and dynamic flexocoupling constants (e.g., f_{11}, f_{44}, and M_{11}) from soft phonon spectra with the assumption of other known material parameters.

Finally, let us answer the question of how important the flexocoupling is for a quantitative description of the observed phonon spectra. In Fig. 4 we compare the paraelectric and ferroelectric soft phonon spectra of $PbTiO_3$ calculated by us with the spectra experimentally observed by Shirane *et al.* [41]**.** Parameters corresponding to the best fitting of $PbTiO_3$ spectra

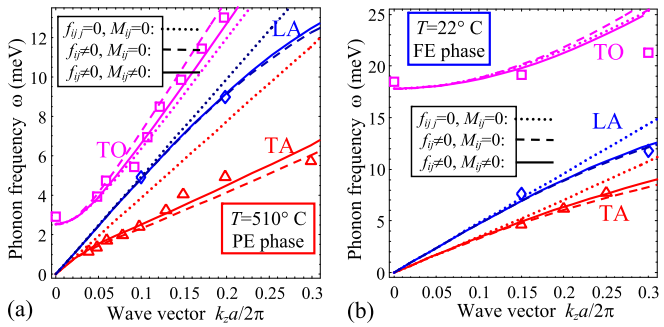

FIG. 4. (Color online) Soft phonon branch frequency vs k calculated in $PbTiO_3$. (a) corresponds to the paraelectric (PE) phase at $T = 510$ C, and (b) is calculated in the ferroelectric (FE) phase ($T = 22$ C) for the case $\vec{k}\uparrow\uparrow\vec{P}_S$. Symbols are experimental data from Ref. [41]. Dotted curves are calculated without flexoelectric coupling (legend "$f_{ij} = 0, M_{ij} = 0$"); dashed curves are calculated with the static but without the dynamic effect (legend "$f_{ij} \neq 0, M_{ij} = 0$"); and solid curves are calculated with the dynamic and static flexoelectric effects included (legend "$f_{ij} \neq 0, M_{ij} \neq 0$"). Parameters corresponding to the best fitting of $PbTiO_3$ spectra are listed in the last row of Table I**.**

are listed in the last column of Table I. It is clear from the figure that only the solid curves calculated for both nonzero static and dynamic flexocoupling constants ($f_{11} = -8\,\mathrm{V}$, $f_{44} = -1.9\,\mathrm{V}$, and $M_{11} = -2 \times 10^{-8}\,\mathrm{V\,s^2/m^2}$) describe quantitatively the observed paraelectric and ferroelectric soft phonon spectra of $PbTiO_3$ at small **k** (compare the dotted, dashed, and solid curves in Fig. 4). Therefore it is hardly possibly to fit the experimental results without inclusion of nonzero static and dynamic flexocoupling constants. Hence we conclude that both these contributions are critically important in a quantitativedescription of the available experimental data even at small k.

V. SUMMARY

Within the Landau-Ginzburg-Devonshire approach we established the impact of the static and dynamic flexocoupling on the correlation function of the long-range order parameter fluctuations in the ferroelectric phase of ferroics with local disordering sources and obtained analytical expressions for the generalized susceptibility and phonon dispersion relations for ferroelectrics with arbitrary symmetry and elastic and electrostrictive anisotropy. Relatively simple analytical expressions for the susceptibility components and soft phonon dispersion law were derived in the cubic approximation for the elastic and electrostrictive properties of ferroelectrics. Using the expressions, we studied the physical manifestations of the flexocoupling and came to the following conclusions:

(a) The joint action of the static and dynamic flexoelectric effects induces nondiagonal components of the generalized susceptibility, whose amplitudes are proportional to the convolution of the spontaneous polarization with the flexocoupling constants.

(b) The flexocoupling essentially broadens the k spectrum of the generalized susceptibility and so decreases the correlation radii.

(c) The contribution of spontaneous polarization via ferroelectric nonlinearity and electrostriction mechanisms can lead to both broadening and narrowing of the k spectrum of the susceptibility.

(d) The appearance of spontaneous polarization leads to the removal of the modes' degeneracy and consequently to the appearance of different transverse acoustic and optical modes. The flexoelectric coupling significantly increases the splitting of the acoustic modes, as well as leading to the additional pushing away of the optical and acoustic soft mode phonon branches.

(e) It appeared hardly possible to fit adequately the experimentally observed phonon spectra of lead zirconate titanate for zero static and dynamic flexocoupling constants even at small k. Hence we conclude that both the static and dynamic contributions are critically important to describe quantitatively the available experimental data.

Also we would like to underline that we did not aim to reach a quantitative agreement between the calculated and experimentally observed soft phonon spectra in the first Brillouin zone. Consideration of the problem for higher **k** values requires including the anharmonicity and higher gradient terms to modify the harmonic approach we used. However, our results prove the evident importance of the static and dynamic flexocouplings for the adequate description of the generalized susceptibilities and soft phonon spectra near the center of the Brillouin zone. Since modern and classic experimental methods readily capture the small-k region, further study of the flexocouplings' impact on the susceptibility spectra for all crystallographic symmetries seems important. Note that our model does not contain any damping, but the energy dissipation (e.g., sound attenuation or optical phonon damping [52]) could also be analyzed with account of flexocoupling on the basis of the Landau-Khalatnikov theory. The results obtained can be extremely important for theoretical analyses of the broad spectrum of experimental data including neutron and Brillouin scattering, which collects unique information from the structural factors and phonon dispersion.

ACKNOWLEDGMENTS

The authors gratefully acknowledge the extremely useful suggestion to include the dynamic flexoelectric coupling into the theoretical consideration and multiple consultations and discussions with Professor A. K. Tagantsev (EPFL). E.A.E. and A.N.M. acknowledge the National Academy of Sciences of Ukraine (Grants No. 35-02-15 and No. 07-06-15) and Center for Nanophase Materials Sciences, user project CNMS 2014-270. M.V.S. acknowledges the Russian Science Foundation (Grant No. 15-19-20038). This research was sponsored by the Division of Materials Sciences and Engineering, BES, DOE (S.V.K.). A portion of this research was conducted at the Center for Nanophase Materials Sciences, which is a DOE Office of Science User Facility.

A.N.M. formulated the theoretical problem, derived general analytical expressions, and wrote the initial text of the manuscript with figures. E.A.E. derived the analytical expressions for cubic symmetry, performed corresponding numerical simulations, and prepared the illustrations jointly with O.V.V. Y.M.V. worked in detail on the improvement, physical interpretation, and correlation with experiment of the obtained theoretical results. M.V.S. and S.V.K., jointly with A.N.M. and Y.M.V., worked on the detailed improvement of the paper's text, discussion, and conclusions.

[1] D. Lee, A. Yoon, S. Y. Jang, J.-G. Yoon, J.-S. Chung, M. Kim, J. F. Scott, and T. W. Noh, Giant Flexoelectric Effect in Ferroelectric Epitaxial Thin Films, Phys. Rev. Lett. **107**, 057602 (2011).

[2] P. V. Yudin and A. K. Tagantsev, Fundamentals of flexoelectricity in solids, Nanotechnology **24**, 432001 (2013).

[3] P. Zubko, G. Catalan, and A. K. Tagantsev, Flexoelectric effect in solids, Annu. Rev. Mater. Res. **43**, 387 (2013).

[4] Kazuhide Abe, Shuichi Komatsu, Naoko Yanase, Kenya Sano, and Takashi Kawakubo. Asymmetric ferroelectricity and anomalous current conduction in heteroepitaxial $BaTiO_3$ thin films, Jpn. J. Appl. Phys. **36**, 5846 (1997).

[5] K. Abe, N. Yanase, T. Yasumoto, and T. Kawakubo, Voltage shift phenomena in a heteroepitaxial $BaTiO_3$ thin film capacitor, J. Appl. Phys. **91**, 323 (2002).

[6] Alexander K. Tagantsev, L. Eric Cross, and Jan Fousek. *Domains in Ferroic Crystals and Thin Films* (Springer, New York, 2010).

[7] G. Catalan, L. J. Sinnamon and J. M. Gregg, The effect of flexoelectricity on the dielectric properties of inhomogeneously strained ferroelectric thin films, J. Phys.: Condens. Matter **16**, 2253 (2004).

[8] G. Catalan, Beatriz Noheda, J. McAneney, L. J. Sinnamon, and J. M. Gregg, Strain gradients in epitaxial ferroelectrics, Phys. Rev. B **72**, 020102 (2005).

[9] E. A. Eliseev, A. N. Morozovska, M. D. Glinchuk, and R. Blinc, Spontaneous flexoelectric/flexomagnetic effect in nanoferroics, Phys. Rev. B **79**, 165433 (2009).

[10] M. S.Majdoub, R. Maranganti, and P. Sharma, Understanding the origins of the intrinsic dead layer effect in nanocapacitors, Phys. Rev. B **79**, 115412 (2009).

[11] Hao Zhou, Jiawang Hong, Yihui Zhang, Faxin Li, Yongmao Pei, and Daining Fang, Flexoelectricity induced increase of critical thickness in epitaxial ferroelectric thin films, Physica B: Condens. Matter **407**, 3377 (2012).

[12] Peter Maksymovych, Anna N. Morozovska, Pu Yu, Eugene A. Eliseev, Ying-Hao Chu, Ramamoorthy Ramesh, Arthur P. Baddorf, and Sergei V. Kalinin, Tunable metallic conductance in ferroelectric nanodomains, Nano Lett. **12**, 209 (2012).

[13] E. A. Eliseev, A. N. Morozovska, G. S. Svechnikov, Peter Maksymovych, and S. V. Kalinin, Domain wall conduction in multiaxial ferroelectrics: impact of the wall tilt, curvature, flexoelectric coupling, electrostriction, proximity and finite size effects, Phys. Rev.B **85**, 045312 (2012)

[14] Albina Y. Borisevich, E. A. Eliseev, A. N. Morozovska, C-J. Cheng, J-Y. Lin, Ying-Hao Chu, Daisuke Kan, Ichiro Takeuchi, V. Nagarajan, and Sergei V. Kalinin, Atomic-scale evolution of modulated phases at the ferroelectric–antiferroelectric morphotropic phase boundary controlled by flexoelectric interaction, Nat. Commun. **3**, 775 (2012).

[15] P. V. Yudin,, A. K. Tagantsev, E. A. Eliseev, A. N. Morozovska, and Nava Setter, Bichiral structure of ferroelectric domain walls driven by flexoelectricity, Phys. Rev. B **86**, 134102 (2012).

[16] Eugene A. Eliseev, Peter V. Yudin, Sergei V. Kalinin, Nava Setter, Alexander K. Tagantsev, and Anna N. Morozovska, Structural phase transitions and electronic phenomena at 180-degree domain walls in rhombohedral $BaTiO_3$, Phys. Rev. B **87**, 054111 (2013).

[17] Anna N. Morozovska, Eugene A. Eliseev, Maya D. Glinchuk, Long-Qing Chen, and Venkatraman Gopalan, Interfacial polarization and pyroelectricity in antiferrodistortive structures induced by a flexoelectric effect and rotostriction, Phys. Rev. B **85**, 094107 (2012).

[18] Eugene A. Eliseev, Anna N. Morozovska, Yijia Gu, Albina Y. Borisevich, Long-Qing Chen, Venkatraman Gopalan, and Sergei V. Kalinin, Conductivity of twin walls–surface junctions in ferroelastics: Interplay of deformation potential, octahedral rotations, improper ferroelectricity, and flexoelectric coupling, Phys. Rev. B **86**, 085416 (2012).

[19] Eugene A. Eliseev, Sergei V. Kalinin, Yijia Gu, Maya D. Glinchuk, Victoria Khist, Albina Borisevich, Venkatraman Gopalan, Long-Qing Chen, and Anna N. Morozovska, Universal emergence of spatially-modulated structures induced by flexo-antiferrodistortive coupling in multiferroics, Phys. Rev. B **88**, 224105 (2013).

[20] M. Gharbi, Z. H. Sun, P. Sharma, and K. White, The origins of electromechanical indentation size effect in ferroelectrics, Appl. Phys. Lett. **95**, 142901 (2009).

[21] M. Gharbi, Z. H. Sun, P. Sharma, K. White, and S. El-Borgi, Flexoelectric properties of ferroelectrics and the nanoindentation size-effect, Int. J. Solids Struct. **48**, 249 (2011).

[22] C. R. Robinson, K. W. White, and P. Sharma, Elucidating the mechanism for indentation size-effect in dielectrics, Appl. Phys. Lett. **101**, 122901 (2012).

[23] A. N. Morozovska, E. A. Eliseev, A. K. Tagantsev, S. L. Bravina, Long-Qing Chen, and S. V. Kalinin, Thermodynamics of electromechanically coupled mixed ionic-electronic conductors: Deformation potential, Vegard strains, and flexoelectric effect, Phys. Rev. B **83**, 195313 (2011).

[24] A. N. Morozovska, E. A. Eliseev, G. S. Svechnikov, and S. V. Kalinin, Nanoscale electromechanics of paraelectric materials with mobile charges: Size effects and nonlinearity of electromechanical response of $SrTiO_3$ films, Phys. Rev. B **84**, 045402 (2011).

[25] H. Lu, C.-W. Bark, D. Esque de los Ojos, J. Alcala, C. B. Eom, G. Catalan, and A. Gruverman. Mechanical writing of ferroelectric polarization, Science **336**, 59 (2012).

[26] V. S. Mashkevich and K. B. Tolpygo, Electrical, optic and elastic properties of crystals of diamond type, Zh. Eksp. Teor. Fiz. **31**, 520 (1957) [Sov. Phys. JETP **4**, 455 (1957)].

[27] Sh. M. Kogan, Piezoelectric effect under an inhomogeneous strain and an acoustic scattering of carriers of current in crystals, Solid State Phys. **5**, 2829 (1963).

[28] A. K. Tagantsev, Piezoelectricity and flexoelectricity in crystalline dielectrics, Phys. Rev. B **34**, 5883 (1986).

[29] W. Ma and L. E. Cross, Strain-gradient-induced electric polarization in lead zirconate titanate ceramics, Appl. Phys. Lett. **82**, 3293 (2003).

[30] P. Zubko, G. Catalan, A. Buckley, P. R. L. Welche, and J. F. Scott, Strain-Gradient-Induced Polarization in $SrTiO_3$ Single Crystals, Phys. Rev. Lett. **99**, 167601 (2007).

[31] W. Ma and L. E. Cross, Flexoelectricity of barium titanate, Appl. Phys. Lett. **88**, 232902 (2006).

[32] W. Ma and L. E. Cross, Flexoelectric effect in ceramic lead zirconate titanate, Appl. Phys. Lett. **86**, 072905 (2005).

[33] I. Ponomareva, A. K. Tagantsev, and L. Bellaiche, Finite-temperature flexoelectricity in ferroelectric thin films from first principles, Phys. Rev. B **85**, 104101 (2012).

[34] Jiawang Hong and David Vanderbilt, First-principles theory of frozen-ion flexoelectricity, Phys. Rev. B **84**, 180101(R) (2011).

[35] Alexander Kvasov and Alexander K. Tagantsev, Dynamic flexoelectric effect in perovskites from first principles calculations, Phys. Rev. B **92**, 054104 (2015).

[36] E. Farhi, A. K. Tagantsev, R. Currat, B. Hehlen, E. Courtens, and L. A. Boatner, Low energy phonon spectrum and its parameterization in pure $KTaO_3$ below 80 K, Eur. Phys. J. B **15**, 615 (2000).

[37] K. F. Astafiev, A. K. Tagantsev, and N. Setter, Quasi-Debye microwave loss as an intrinsic limitation of microwave performance of tunable components based on $SrTiO_3$ and $Ba_xSr_{1-x}TiO_3$ ferroelectrics, J. Appl. Phys. **97**, 014106 (2005).

[38] W. Cochran, Dynamical, scattering and dielectric properties of ferroelectric crystals, Adv. Phys. **18**, 157 (1969).

[39] J. Hlinka, I. Gregora, and V. Vorlıcek, Complete spectrum of long-wavelength phonon modes in $Sn_2P_2S_6$ by Raman scattering, Phys. Rev. B **65**, 064308 (2002).

[40] R. M.Yevych, Yu. M. Vysochanskii, M. M. Khoma, and S. I. Perechinskii, Lattice instability at phase transitions near the Lifshitz point in proper monoclinic ferroelectrics, J. Phys.: Condens. Matter **18**, 4047 (2006).

[41] G. Shirane, J. D. Axe, J. Harada, and J. P. Remeika, Soft ferroelectric modes in lead titanate, Phys. Rev. B **2**, 155 (1970).

[42] G. Shirane, J. D. Axe, J. Harada, and A. Linz, Inelastic neutron scattering from single-domain $BaTiO_3$, Phys. Rev. B **2**, 3651 (1970).

[43] G. Shirane, B. C. Frazer, V. J. Minkiewicz, J. A. Leake, and A. Linz, Soft Optic Modes in Barium Titanate, Phys. Rev. Lett. **19**, 234 (1967).

[44] A. K. Tagantsev, and G. Gerra, Interface-induced phenomena in polarization response of ferroelectric thin films, J. Appl. Phys. **100**, 051607 (2006).

[45] See Supplemental Materials at http://link.aps.org/supplemental/10.1103/PhysRevB.92.094308 for details of calculation.

[46] J. D. Freire, and R. S. Katiyar, Lattice dynamics of crystals with tetragonal $BaTiO_3$ structure, Phys. Rev. B **37**, 2074 (1988).

[47] H. B. Callen and T. A. Welton, Irreversibility and generalized noise, Phys. Rev. **83**, 34 (1951).

[48] P. V. Yudin, R. Ahluwalia, and A. K. Tagantsev, Upper bounds for flexocoupling coefficients in ferroelectrics, Appl. Phys. Lett. **104**, 082913 (2014).

[49] M. J. Haun, Z. Q. Zhuang, E. Furman, S. J. Jang, and L. E. Cross, Thermodynamic theory of the lead zirconate-titanate solid solution system, part III: Curie constant and sixth-order polarization interaction dielectric stiffness coefficients, Ferroelectrics **99**, 45 (1989).

[50] N. A. Pertsev, V. G. Kukhar, H. Kohlstedt, and R. Waser, Phase diagrams and physical properties of single-domain epitaxial Pb $(Zr_{1-x}Ti_x)O_3$ thin films, Phys. Rev. B **67**, 054107 (2003).

[51] M. J. Haun, E. Furman, S. J. Jang, H. A. McKinstry, and L. E. Cross, Thermodynamic theory of $PbTiO_3$, J. Appl. Phys. **62**, 3331 (1987).

[52] A. A. Kohutych, R. M. Yevych, S. I. Perechinskii, and Y. M. Vysochanskii, Acoustic attenuation in ferroelectric $Sn_2P_2S_6$ crystals, Open Physics **8**, 905 (2010).